Design of Defective EBG Structures for Dual-Band Circular Patch MIMO Antenna Applications

Xiaoyan Zhang [1,2], Yuting Chen [1*], Haitao Ma [1], Liwei Li [1], and Huihui Xu [1]

[1] School of Information Engineering
East China Jiaotong University, Nanchang, 330013, China
xyzhang3129@ecjtu.jx.cn, *cytzgao@qq.com, 2538338841@qq.com,
liliwei_139@163.com, 164449524@qq.com

[2] State Key Laboratory of Millimeter Waves, Nanjing, 210096, China

Abstract ─ Usually, a reasonably designed electromagnetic band-gap (EBG) structure can reduce the surface wave of an antenna. However, it may take a long time to design. In this paper, a dual-band circular patch multiple-input multiple-output (MIMO) antenna on an EBG surface is proposed. Defects are simply introduced into rows and columns of the EBG cells. In this way, the band-gap bandwidth (BG-BW) of those cells can be as large as 29.2%, which enables the EBGs can cover two frequency bands with a large interval, and to generate over 25 dB isolation between the antenna elements, as well. The measured results show that the proposed antenna, incorporating defective EBGs, operates at 5.71-5.97 GHz and 6.31-6.54 GHz. The -10 dB impedance bandwidth of the antenna is extended by 28.9% and 27.8% at the low and high frequency band. In addition, its gain is enhanced by 5 dB and 6.9 dB, and its back radiation decreased by 15 dB and 10.3 dB at the resonant frequencies of 5.75 GHz and 6.44 GHz, respectively. The proposed design may have many applications in communication systems.

Index Terms ─ Defect, high impedance EBG structure, MIMO antenna, mushroom EBG structure.

I. INTRODUCTION

In recent years, multiple-input multiple-output (MIMO) technology has gained a lot of attention from scholars in the telecommunication industry, which is one of the ways to realize the 5-generation mobile communication [1, 2]. The antenna array is an important part of MIMO system. The main challenge in designing MIMO antennas is to improve the isolation between antenna elements while minimizing them as much as possible [3-5]. Generally, the smaller isolation between antennas, the smaller mutual coupling effects on them. For some special antennas, such as base station antennas, the isolation requirement is greater than 25 dB [6].

Some methods were proposed to improve the isolation between antenna elements. Ismaiel and Abdel-Rahman etched meander slots on the ground to improve the isolation [7], but it causes the frequency offset. Yu *et al.* inserted an offset circuit between feed ports [8]. However, this method will increase the complexity of the antenna design. Wang *et al.* added two pairs of *L*-shaped extensions to the background structure of the antenna [9], while the isolation is only 15 dB.

In recent years, electromagnetic band-gap (EBG) structure has been proposed to isolate antennas due to its ease of design and beneficial to reducing an antenna profile. Coulombe *et al*. embedded some coplanar EBG structures to an antenna array [10], its isolation is better than 25 dB. Qiu *et al.* introduced a perpendicular mushroom-like EBG wall to the substrate between the two patch antennas to obtain 30 dB isolation [11]. Although it is not suitable for low profile requirements, it provides a superior idea for antenna isolation design.

It is found that the wider band gap of the EBG structure, the higher isolation of the antennas. The mushroom-like EBG are usually arranged in a periodic [12] or quasi-periodic form [13]. It has many derivative structures, including a two via slot-type EBG (TVS-EBG) [14], an edge-located via EBG (ELV-EBG) [15], a modified mushroom-like EBG (MML-EBG) [16], and a complementary split ring resonator EBG (CSRR-EBG) [17]. The former two adopt the way of changing feed to improve the band-gap bandwidth (BG-BW) of the EBGs, while the latter two achieve this goal by carefully designing the shapes of the cells. Their BG-BWs comparisons are listed in Table 1. It is shown that the latter method can broaden the bandwidth more effectively. However, it may take a long time to design. In 2018, we tried to destroy the periodicity of the EBGs by introducing some defective slots only between the rows of the EBG cells to obtain a higher BG-BW [18], but the band gap was still not wide enough.

Submitted On: October 12, 2018
Accepted On: January 26, 2019

In this paper, a dual-band circular patch MIMO antenna with defective EBGs is proposed. The design of EBG structure is based on mushroom-like EBG structure that digs four half circular slots. And the defects are introduced into both rows and columns of the EBG cells. By using the proposed EBG, the bandwidth and gain can be dramatically improved.

Table 1: The lowest frequency (f_L), highest frequency (f_H) and band-gap bandwidth in different EBG structures

Ref.	Type	f_L (GHz)	f_H (GHz)	BG-BW
[14]	TVS-EBG	3.01	3.38	11.6%
[15]	ELV-EBG	3.60	4.06	12.0%
[16]	MML-EBG	5.10	6.00	16.2%
[17]	CSRR-EBG	3.31	4.33	26.7%
Proposed	—	5.68	7.62	29.2%

II. DESIGN AND ANALYSIS

A. Dual-band circular patch MIMO antenna design

Figure 1 shows a circular patch MIMO antenna in the C-band. The MIMO antenna is designed on a FR-4 substrate, whose thickness is h=2 mm and the electrical parameters are ε_r=4.4 and $tan\delta$ =0.02. The MIMO antenna is a circle patch and the radius of the circular patch is 11.5 mm. As Fig. 1 shows, the lengths and widths of slots are denoted by l_1, l_2, l_3, l_4, l_5, l_6, l_7, and d, respectively. The center of the circle patch is denoted by r_1. This antenna is excited by a coaxial cable with a 50 Ω SMA connector, it has a diameter of r_2=1 mm. The two elements of MIMO antenna distance is d_y.

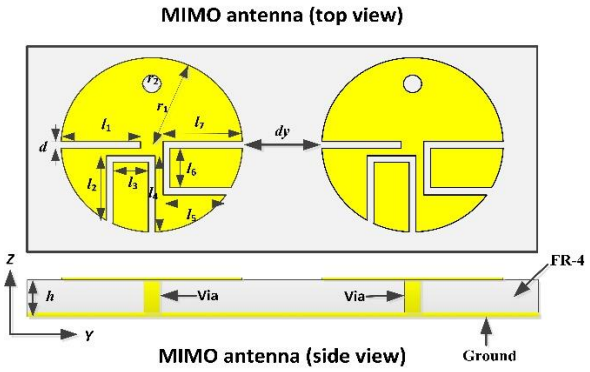

Fig. 1. Configuration and parameters of circular patch MIMO antenna and substrate, for MIMO antenna: l_1=10.5 mm, l_2=7 mm, l_3=8 mm, l_4=10 mm, l_5=7 mm, l_6=8 mm, l_7=10mm, d=0.5 mm, r_1=11.5 mm, r_2=1 mm, d_y=33.6 mm, and h=2 mm.

Figure 2 exhibits the simulated S_{11} of circular patch MIMO antenna. The MIMO antenna has two resonant modes generated at nearly 5.75 GHz and 6.44 GHz, respectively. Its bandwidth is 320 MHz at lower frequency and 200 MHz at higher frequency with a standard of S_{11} < -10 dB. The radiation efficiency of this antenna is about 73.9% at 5.75 GHz and 70.5% at 6.44 GHz, respectively.

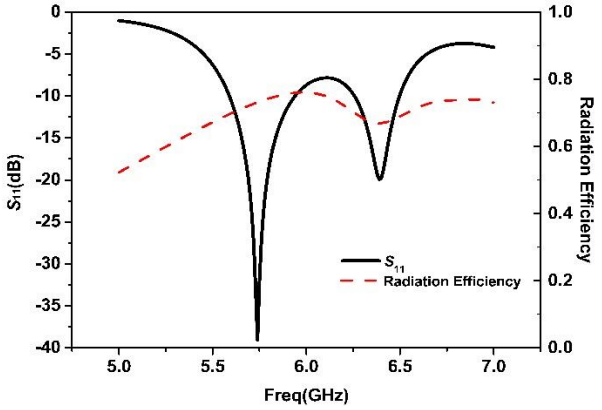

Fig. 2. S_{11} and radiation efficiency of the MIMO antenna.

B. High impedance EBG structure design

Figure 3 (a) shows the schematic of the high impedance EBG in three different cases. EBG has thickness of 2 mm with a dielectric constant of 4.4. Figure 3 (b) shows the 1×2 EBGs structure proposed. Figure 3 (c) presents the 10×16 EBG cells operating as a two-port waveguide formed by a pair of perfect electric conductor (PEC) along the z-axis and perfect magnetic conductor (PMC) along the y-axis. They are divided into seven parts: #1, #2, #3, #4, #5, #6, and #7. By changing the distances of g_x, g_y, and g_z between each part, the asymmetrically distribution of EBGs can be realized. Besides, when g_x and g_y equals dx, the EBGs are periodically arranged.

Figure 4 shows that the EBG structure can be equivalent to parallel LC resonant circuit. The gap between radiation patches of adjacent EBG structures can be equivalent to capacitance C. Because the metal through-hole connects the radiation patch with the ground structure, the current forms a loop between the radiation patch and the ground structure, which can be equivalent to the inductance L. This high impedance surface (HIS) can effectively suppress the surface wave outside the band-gap. For an EBG structure with patch width W, gap width g, substrate thickness h, the values of the L and C are determined by the following formula [19]:

$$L = \mu_0 h, \tag{1}$$

$$C = \frac{W\varepsilon_0(1+\varepsilon_r)}{\pi} cosh^{-1}\left(\frac{2W+g}{g}\right), \tag{2}$$

where ε_r is the electric constant, while ε_0 and μ_0 is the permittivity and permeability of free space, respectively.

The frequency band gap also can be predicted as:

$$\omega = 1/\sqrt{LC}, \quad (3)$$

$$\mathrm{BW} = \Delta\omega/\omega = 1/\eta\sqrt{L/C}, \quad (4)$$

where η is the free space impedance, which is 120 π.

Based on the above formulas, L is proportional to h, the band gap increases with the increasing of L, and decreases with the decreasing of L when μ_0 and η_0 are constant. W will affect the value of C when other variables are fixed. C is inversely proportional to the value of the band gap.

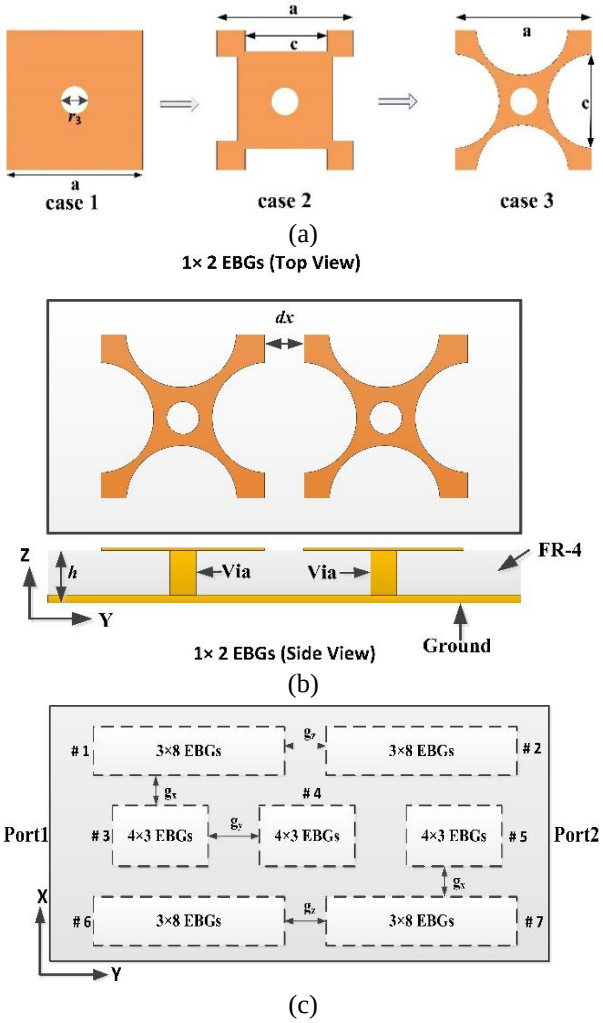

Fig. 3. (a) Configuration and parameters of the proposed EBG for high impedance EBG in the three different cases: a=6.3 mm, c=3.4 mm, r_3=1 mm, for 1×2 EBGs: dx=0.5 mm, h=2 mm; for 10×16 EBGs: g_x=5 mm, g_y=36.7 mm, and g_z=2.7 mm. (a) EBG cell in three different cases, (b) 1×2 EBGs structure, and (c) 10×16 EBGs structure.

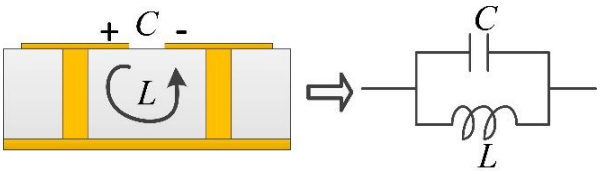

Fig. 4. Two-dimensional model for mushroom EBG type.

Figure 5 displays the effect of the slots above the electromagnetic band-gap for three cases. As seen in the above figures, under the condition of the same size, by etching circle slots on the case 3, the bandwidth of EBG is the largest. Figure 6 presents the S_{21} of proposed EBG structure. While, when g_x, g_y, and $g_z > dx$, the band-gap is broadened, because the EBG periodical structure is broken [18].

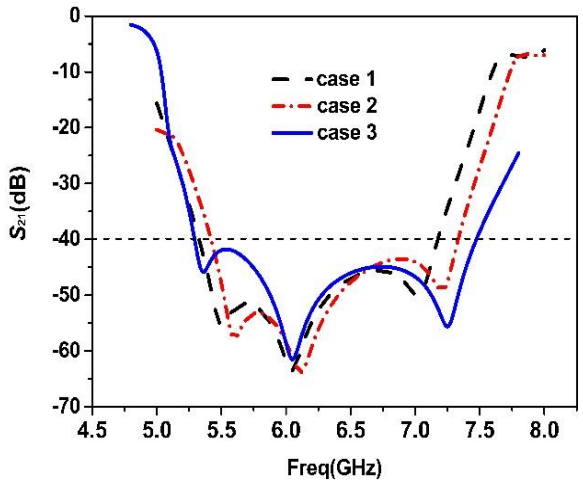

Fig. 5. Simulated S_{21} of case 1, case 2, and case 3.

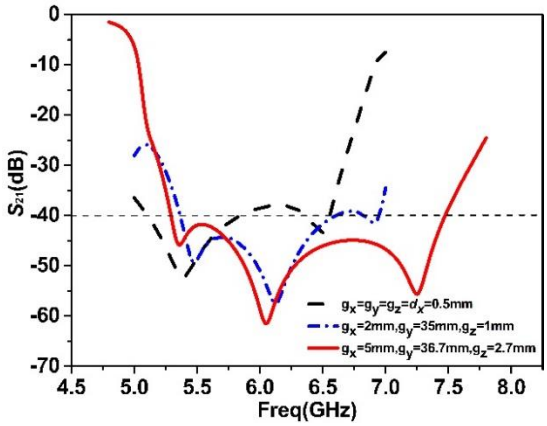

Fig. 6. S_{21} of the proposed EBG structure.

The dispersion diagrams are plotted in Fig. 7. From this diagram, the frequency band-gap between mode 1 and mode 2 is observed for the proposed EBG cell. The intersections with the light lines are used to determine the upper limit of the band-gap for the surface waves. Case 3 is proposed, the frequency of electromagnetic band gaps of the EBG structure is 5.68 GHz to 7.62 GHz, and the band gaps are 1.94 GHz.

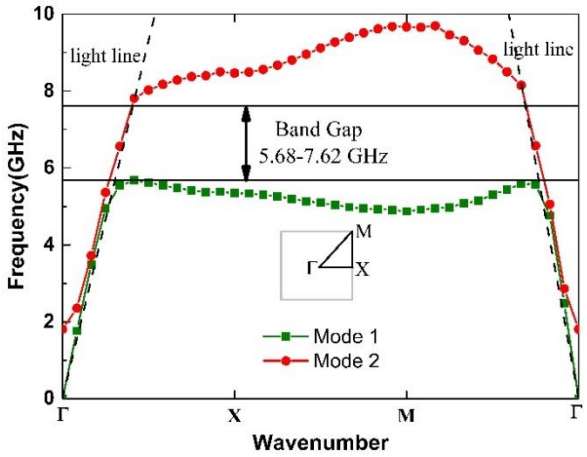

Fig. 7. Dispersion diagram for case 3.

C. A dual-band circular patch MIMO antenna with high impedance EBG structure

Figure 8 demonstrates the configuration and parameters of the proposed EBG antenna. The d_1 and d_2 equal 6.85 mm, the *Width* is 80 mm and *Length* is 135 mm.

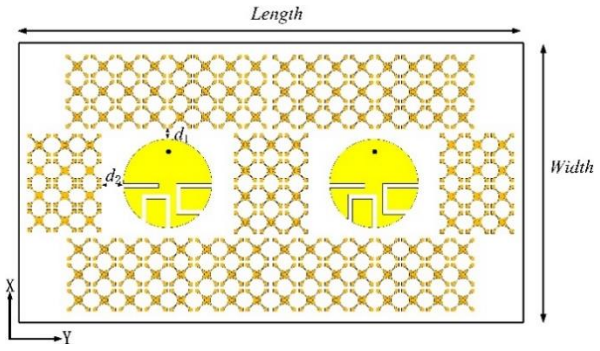

Fig. 8. Configuration and parameters of the proposed EBG antenna.

Figure 9 shows the S_{11} of the proposed EBG antenna. As can be observed, the EBG antenna bandwidth is 5.6 GHz to 6.0 GHz and 6.22 GHz to 6.46 GHz, respectively. The bandwidth is 400 MHz in low frequency and 240 MHz in high frequency, respectively. The radiation efficiency of proposed antenna is about 61.1% at 5.75 GHz and 56.1% at 6.44 GHz. Figure 10 shows the current distributions of proposed EBG antenna. It demonstrates that the proposed EBG structure can more obviously suppress the surface wave of the antenna. The radiation of the EBG antenna is clearly stronger than that of the MIMO antenna.

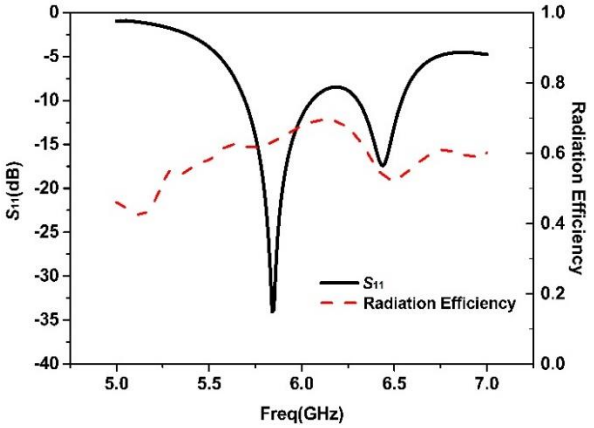

Fig. 9. S_{11} and radiation efficiency of the proposed EBG antenna.

For a MIMO antenna system, the isolation is an important parameter. It can be described as $|S_{21}|$. Figure 11 presents a slot in the ground planar of the MIMO antenna. The length and width of the slot are expressed by *glength* and *gwidth*, respectively. The MIMO antenna observed the isolation by changing the size of slot. When the *glength* equals 50 mm and *gwidth* equals 1.5 mm, the isolation of MIMO antenna can reach maximum.

Figure 12 compares the mutual coupling of the proposed EBG antenna with the MIMO antenna and slot in ground. It is shown that the proposed EBG structure is more significant in improving the mutual coupling of MIMO antenna system compared with slot in ground. Especially, at low frequency, the isolation can be enhanced by about 11.5 dB with EBG than about 0.3 dB with slot line.

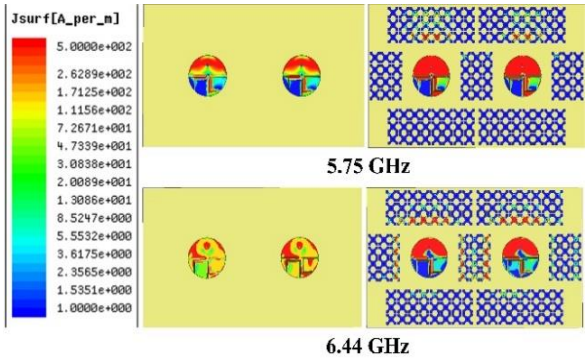

Fig. 10. Current distributions of MIMO antenna and the proposed EBG antenna at 5.75 GHz and 6.44 GHz.

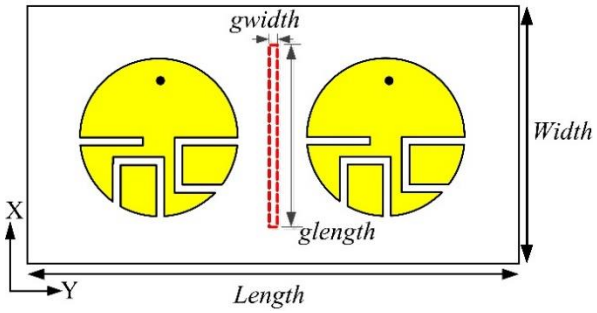

Fig. 11. Slot in ground planar of MIMO antenna.

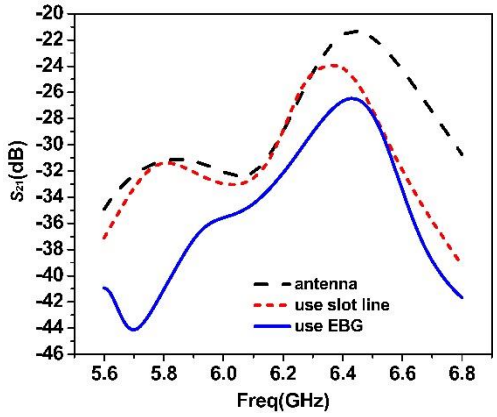

Fig. 12. Simulated isolation ($|S_{21}|$) of the proposed EBG antenna.

III. EXPERIMENTAL RESULTS AND DISCUSSION

Figure 13 depicts the photographs of the fabricated EBG antenna. Figure 14 shows the measured S_{11} of the MIMO antenna and proposed EBG antenna. The measured results show that -10 dB impedance bandwidth of the MIMO antenna is 4.5% (5.71-5.97 GHz) at the lower band and 3.6% (6.31-6.54 GHz) at the high band. When EBGs are asymmetrically arranged, the frequency bands become 5.8% (5.7-6.04 GHz) and 4.6% (6.30-6.60 GHz). Compared to the MIMO antenna, the bandwidth of proposed EBG antenna is extended by 28.9% in low frequency and 27.8% in high frequency, respectively.

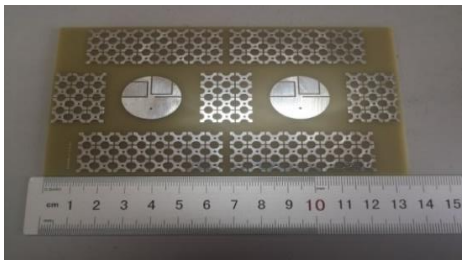

Fig. 13. Photographs of the fabricated EBG antenna.

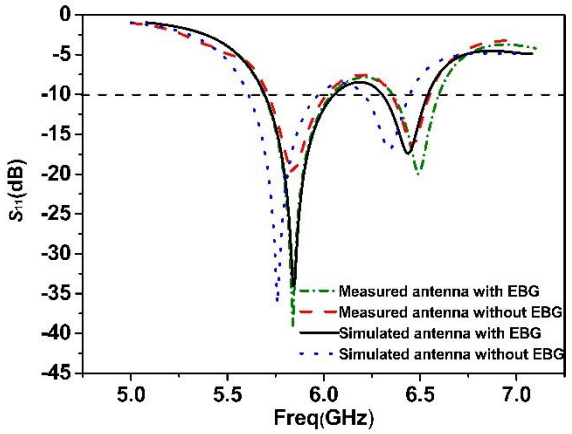

Fig. 14. Measured and simulated S_{11} of the antenna with or without EBG.

As Fig. 15 shows, when the frequency is 5.75 GHz, the gain of EBG antenna is 7 dB and the back radiation is -25 dB. The gain of MIMO antenna is 2 dB and the back radiation is -10 dB. Compared with the MIMO antenna, the gain of EBG with antenna is increased by 5 dB and the back radiation is decreased 15 dB in the E-plane. It is also shown that the cross-polarization is low at low frequency and the simulation results are basically consistent with the measured results. Figure 16 shows the gain of proposed EBG antenna is 8 dB and its back radiation is -20.5 dB at 6.44 GHz. While, the gain of traditional MIMO antenna is 1.1 dB with -10.2 dB back radiation. Compared with MIMO antenna, the gain of EBG antenna is added 6.9 dB and the back radiation is reduced 10.3 dB in the E-plane. The radiation patterns of the cross-polarization get worse at 6.44 GHz than at 5.75 GHz. There are some differences between the test results and the simulation results due to its fabrication tolerance.

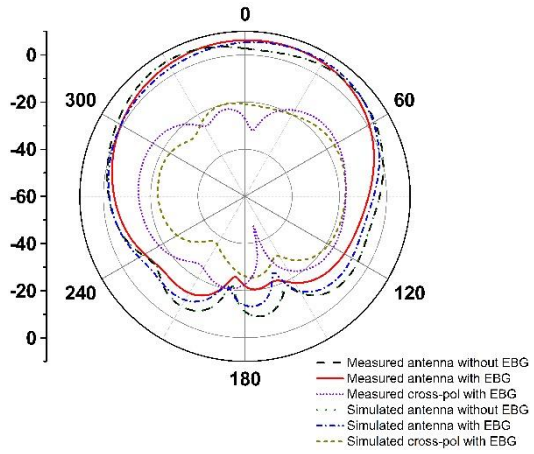

Fig. 15. Measured and simulated E-plane radiation patterns of the antenna at 5.75 GHz.

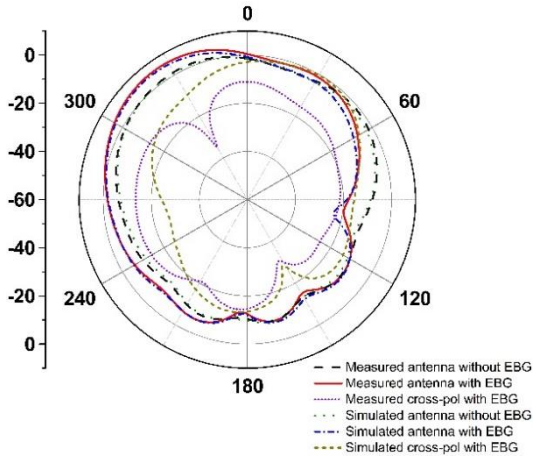

Fig. 16. Measured and simulated E-plane radiation patterns of the antenna at 6.44 GHz.

Figure 17 presents the measured and simulated isolation ($|S_{21}|$) of the proposed EBG antenna compared with MIMO antenna. The measured average isolation is around 43 dB at low frequency and 26 dB at high frequency band. Compared with the MIMO antenna, the isolation of EBG antenna is significantly improved and the measured results are in good agreement with the simulated results.

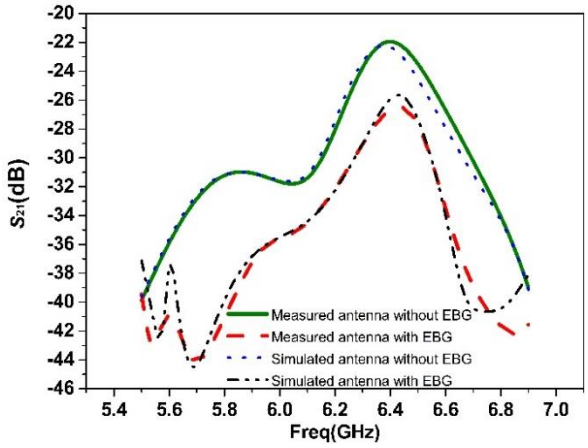

Fig. 17. Measured and simulated isolation ($|S_{21}|$) of proposed EBG antenna compared with MIMO antenna.

IV. CONCLUSION

A dual-band circular patch MIMO antenna with defective EBG structure is proposed. First and foremost, the MIMO antenna resonates at around 5.75 GHz and 6.44 GHz, the frequency covers 5.71 GHz to 5.97 GHz and 6.31 GHz to 6.54 GHz, respectively. Moreover, a high impedance EBG structure is proposed, the band gap of EBG structure is 5.68 GHz to 7.62 GHz. It can cover the frequency of the MIMO antenna. Last but not least, three rows of high impedance EBG cells are designed on the substrate to surround the MIMO antenna. By breaking the periodicity of the EBG structure, the performance parameters of the antenna will be better. The EBG with antenna has a wider bandwidth, which is extended 28.9% in low frequency and 27.8% in high frequency, respectively. In addition, the minimum isolation of the antenna is 26 dB.

The proposed EBG antenna has a higher gain and lower back radiation. When the frequency is 5.75 GHz, the gain of EBG antenna is increased 5 dB and back radiation is reduced 15 dB in the E-plane. In the H-plane, the gain of EBG antenna is increased 5 dB and back radiation is reduced 15 dB. When the frequency is 6.44 GHz, the gain of EBG antenna is increased 6.9 dB and back radiation is reduced 10.3 dB in the E-plane. In the H-plane, the gain of EBG with antenna is increased 4.5 dB and back radiation is decreased 7.7 dB. From the above results, the performance parameters of the proposed EBG antenna have been significantly improved and have a reasonable design.

ACKNOWLEDGE

The authors wish to acknowledge the supports of National Natural Science Foundation of China through Grant #61761017, #61561021, Open Project of State Key Laboratory of Millimeter Wave through Grant #K201829.

REFERENCES

[1] T. L. Marzetta, "Noncooperative cellular wireless with unlimited numbers of base station antennas," *IEEE Transactions on Wireless Communications*, vol. 9, no. 11, pp. 3590-3600, 2010.

[2] F. Rusek, D. Persson, B. K. Lau, and E. G. Larsson, "Scaling up MIMO: Opportunities and challenges with very large arrays," *IEEE Signal Processing Magazine*, vol. 30, no. 1, pp. 40-60, 2013.

[3] S. W. Su, "High-gain dual-loop antennas for MIMO access points in the 2.4/5.2/5.8 GHz bands," *IEEE Transactions on Antennas and Propagation*, vol. 58, no. 7, pp. 2412-2419, 2010.

[4] A. Al-Rawi, A. Hussain, J. Yang, M. Franzén, C. Orlenius, and A. A. Kishk, "A new compact wideband MIMO antenna—the double-sided tapered self-grounded monopole array," *IEEE Transactions on Antennas and Propagation*, vol. 62, no. 6, pp. 3365-3369, 2014.

[5] H. Li, L. Kang, Y. Xu, and Y. Z. Yin, "Planar dual-band WLAN MIMO antenna with high isolation," *Applied Computational Electromagnetics Society (ACES) Journal*, vol. 31, no. 12, pp. 1410-1415, Dec. 2016.

[6] X. Y. Zhang, G. Yang, X. R. Wang, and B. C. Li, "A dual-band and dual-polarized antenna array for 2G/3G/LTE base stations," *International Journal of RF and Microwave Computer-aided Engineering*, vol. 26, pp. 154-163, 2016.

[7] A. M. Ismaiel and A. B. Abdel-Rahman, "A meander shaped defected ground structure (DGS) for reduction of mutual coupling between microstrip antennas," *31st National Radio Science Conference (NRSC)*, Cairo, pp. 21-26, 2014.

[8] J. C. Coetzee and Y. Yu, "Design of decoupling networks for circulant symmetric antenna arrays," *IEEE Antennas and Wireless Propagation Letters*, vol. 8, no. 4, pp. 291-294, 2009.

[9] Y. Wang and Z. Du, "A printed dual-antenna system operating in the GSM1800 / GSM1900 / UMTS / LTE2300 / LTE2500 / 2.4-GHz WLAN bands for mobile terminals," *IEEE Antennas and Wireless Propagation Letters*, vol. 13, no. 1, pp. 233-236, 2014.

[10] M. Coulombe, S. F. Koodiani, and C. Caloz, "Compact elongated mushroom (EM)-EBG structure for enhancement of patch antenna array performances," *IEEE Transactions on Antennas and Propagation*, vol. 58, no. 4, pp. 1076-1086, 2010.

[11] L. Qiu, F. Zhao, K. Xiao, S. L. Chai, and J. J. Mao, "Transmit–receive isolation improvement of antenna arrays by using EBG structures," *IEEE Antennas & Wireless Propagation Letters*, vol. 11, no. 11, pp. 93-96, 2012.

[12] Z. J. Han, W. Song, and X. Q. Sheng, "Gain enhancement and RCS reduction for patch antenna by using polarization-dependent EBG surface," *IEEE Antennas and Wireless Propagation Letters*, vol. 16, pp. 1631-1634, 2017.

[13] Y. Liu, Y. W. Hao, and S. X. Gong, "Low-profile high-gain slot antenna with Fabry-Pérot cavity and mushroom-like electromagnetic band gap structures," *Electronics Letters*, vol. 51, no. 4, pp. 305-306, 2015.

[14] P. P. Bhavarthe, S. S. Rathod, and K. T. V. Reddy, "A compact two via slot-type electromagnetic band gap structure," *IEEE Microwave and Wireless Components Letters*, vol. 27, no. 5, 2017.

[15] E. Rajo-Iglesias, L. Inclan-Sanchez, J. L. Vazquez-Roy, and E. Garcia-Munoz, "Size reduction of mushroom-type EBG surfaces by using edge-located vias," *IEEE Microwave and Wireless Components Letters*, vol. 17, no. 9, pp. 670-672, 2007.

[16] A. Mousazadeh and G. H. Dadashzadeh, "A novel compact UWB monopole antenna with triple band-notched characteristics with EBG structure and two folded V-slot for MIMO/Diversity applications," *Applied Computational Electromagnetics Society (ACES) Journal*, vol. 31, no. 1, pp. 1-7, Jan. 2016.

[17] L. Peng, C. L. Ruan, and Z. Q. Li, "A novel compact and polarization dependent mushroom-type EBG using CSRR for dual/triple-band applications," *IEEE Microwave and Wireless Components Letters*, vol. 20, no. 9, pp. 489-491, 2010.

[18] X. Y. Zhang, H. T. Ma, A. Y. Zhan, L. F. Liu, Y. Xie, Y. Q. Yu, and H. W. Liu, "Design of defective electromagnetic band-gap structures for use in dual-band patch antennas," *International Journal of RF and Microwave Computer-aided Engineering*, 2018.

[19] F. Yang and Y. Rahmat-Samii, "Microstrip antennas integrated with electromagnetic band-gap (EBG) structures: A low mutual coupling design for array applications," *IEEE Transactions on Antennas and Propagation*, vol. 51, no. 10, pp. 2936-2946, 2003.

Xianyan Zhang received the B.S. degree in Applied Physics and M.S. degree in Physical Electronics from Yunnan University, Kunming, China, in 2001 and 2004 respectively, and the Ph.D. degree in Electromagnetic Field and Microwave Technology from Institute of Electronics, Chinese Academy of Sciences in 2007. Her research interests include electromagnetic computation, antenna design and wireless power transmission structure design.

Yuting Chen received the B.S. degree in School of Information Engineering from East China Jiaotong University, Nanchang, China, in 2013, and the M.S. degree in Information and Communication Engineering from East China Jiaotong University, Nanchang, China, in 2019. His research interests include electromagnetic band-gap structure, antenna design.

Haitao Ma received the B.S. degree in Applied Electronic Information Engineering from Haikou College of Economics, Haikou, China, in 2015, and the M.S. degree in Vomputer Technology from East China Jiaotong University, Nanchang, China, in 2018. His research interests also include electromagnetic band-gap structure, antenna design.

Liwei Li received the B.S. degree in Communication Engineering from Xingtan College of Qufu Normal University, Jinan, China. She is currently studying at School of Information Engineering, East China Jiaotong University. Her research interests focus on computational electromagnetic.

Huihui Xu received the B.S. degree in Communication Engineering from Chaohu University, Hefei China. She is currently studying at School of Information Engineering, East China Jiaotong University. Her research interests focus on antenna design.